Optimum Design of Broad-Beam Microstrip Reflectarray

PIYAPORN KRACHODNOK AND RANGSAN WONGSAN
School of Telecommunication Engineering, Institute of Engineering
Suranaree University of Technology
111 University Avenue, Muang District, Nakhon Ratchasima, 30000
THAILAND

Abstract: The reflectarray's elements arrangement for generating an arbitrary phase distribution in the antenna aperture and thus a wide beamwidth of far field pattern are presented. The desired phase delay of reflectarray elements, which are duplicated the same radiating aperture as parabolic backscatters, are determined on the construction of the curvature of a shaped backscatter surface with the help of Snell's law for beam forming to cover a broad area. The method of moment (MoM) and the infinite-array are applied to calculate reflection phase characteristic. The optimized feed distance is calculated from the aperture efficiency with considering feed blockage efficiency and has investigated the influence of the feed position on the -3 dB beamwidth and gain performance. Having confirmed the validity of this approach, the X-band antenna prototype is designed and developed. This reflectarray is tested experimentally and shows good performance.

Key-Words: - reflectarray, phase array, broad-beam antenna

1 Introduction

In the wireless communication applications such as the large-scale indoor base station of wireless local area network (WLAN) system, it is desirable for antenna beam to cover a broad area. Therefore, the widely circular beam antenna is an alternative for WLAN applications as shown in Fig.1. The related literatures have been reported by several authors. Smulders *et al.*[1] presented the design of a 60 GHz shaped reflector antenna for WLAN access points by using backscatter reflector, which fabricated from the modified parabolic surface. Also, Wongsan and Thaivirot [2] presented the synthesis of radiation patterns of the variety of shaped backscatters to provide the wide beam for indoor WLAN applications. From these papers, the backscatters have been fabricated from the circular metal sheet that their surfaces are shaped to be geometric curvature. In case of WLAN systems, such antennas are improper because their structures suffer from mechanical drawbacks such as bulkiness and the need for an expansive custom mold for each coverage specification.

Recently, a microstrip reflectarray that combines some of the best feature of microstrip arrays and parabolic reflector was presented in [3]-[9]. The reflectarray antenna consists of a flat reflecting surface and an illuminating feed as shown in Fig.2. On the reflecting surface, there are many isolated elements (e.g. printed patches, dipoles, or rings), which array on flat PCB without any power division transmission lines. A reflectarray configuration is attractive because it allows a single mechanical design to be used repeatedly for a wide variety of different coverage specifications without the need for expensive fabrication of a new mold. The only changes are required that the printed reflecting element dimensions can be changed for each design in order to generate the different beams. Thus, many of the high recurring costs associated with shaped-reflector antennas can be eliminated with flat printed reflectarray [6]. The flat geometry of a reflectarray also lends itself to easier placement and deployment on the WLAN large-scale indoor base station and also in terms of manufacture. In addition, a flat

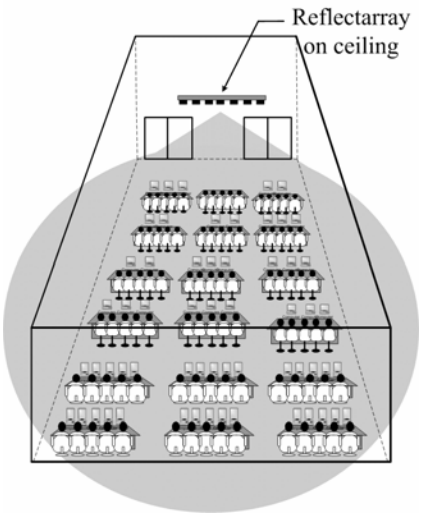

Fig. 1 Reflectarray for WLAN large-scale indoor base station.

printed reflectarray fulfils the antenna requirements for low profile and light weight.

This paper proposes a microstrip reflectarray antenna using parabolic backscatter function to form a wide beam antenna. An effective technique for optimum reflectarray design is to use the aperture efficiency with considering feed blockage efficiency and has investigated the influence of the feed position on the -3 dB beamwidth and gain performance. To achieve such broad-beamwidth, phase of each array element in the reflectarray antenna is designed specifically to emulate the curvature of the backscatter function by using patches of different sizes [7].

The first section, we will present the general design approach as far as it concerns the reflection phase characteristic (Section 2) that describes the desired phase delay of reflectarray elements and the phase calibration technique by using a full-wave method of moment and the infinite-array. In Section 3, we apply this approach to calculate the radiation pattern of the proposed antenna. Design considerations of broad-beam microstrip reflectarray and experimental results are described in Section 4. Finally, the conclusions are given in Section 5.

2 Reflection Phase Characteristic

2.1 Required Phase Delay

Fig. 2 illustrates the incidence of wave on the surface of an analysis model of printed microstrip reflectarray, which parameters used in this figure are described below:

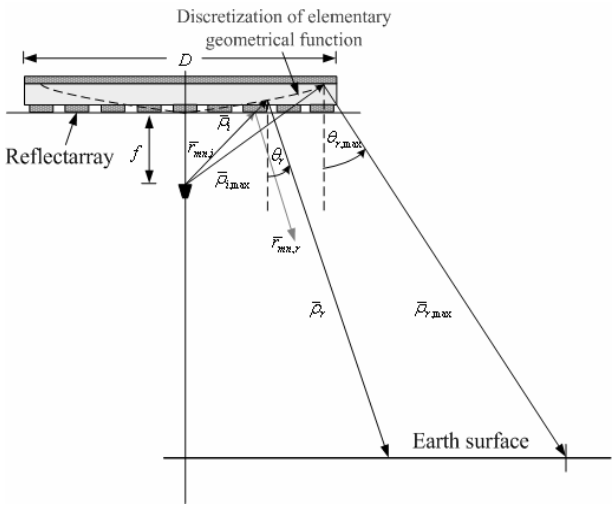

Fig. 2 Analysis model of broad-beam microstrip reflectarray.

$\vec{r}_{mn,i}$ the vector from the feed to the *mn*-th reflectarray element, which can be obtained by using flat geometry;

$\vec{r}_{mn,r}$ the reflected vector from the reflectarray surface to far-field;

$\vec{\rho}_i$ the vector from the feed to the shaped reflector surface, which can be obtained by using curvature geometry;

$\vec{\rho}_r$ the reflected vector from the shaped reflector surface to far-field;

θ_i incidence angle;

θ_r reflection angle;

D dimension of the reflector;

f distance between the feed and the center of the reflectarray.

In general, the feed may be positioned at distance from the reflectarray. The path lengths from the feed to all reflectarray elements are all different, which lead to different phase delays. In this paper, the desired phase delay is determined on the construction of the curvature of a shaped backscatter surface with the help of Snell's law. The relations of the microstrip reflectarray surface to the shape of backscatter are two coordinate systems in this figure: one describes the coordinates (x_r, y_r, z_r) of the reflectarray and the other one describes the coordinate (x_b, y_b, z_b) of the backscatter. The selected shaped reflector is determined by using functions of elementary geometric $(f(z'))$ that aperture cross sections of all backscatters are confined to be circular, same diameter, and very small radius of point source. Since the reflectarray is designed, the following coordinate is used to find the point on the backscatter surface at a given patch element position on the reflectarray as given by (1).

$$\begin{aligned} x_b &= x_r + \left| f(z') - z_r \right| \tan\theta_i \cos\phi_i, \\ y_b &= y_r + \left| f(z') - z_r \right| \tan\theta_i \sin\phi_i, \end{aligned} \tag{1}$$

where the phase center of the feed is located at $(0,0,0)$ and the incidence angle can be described in terms of geometrical dimensions

$$\theta_i = \tan^{-1}\left[\frac{\sqrt{x_r^2 + y_r^2}}{f}\right], \tag{2}$$

$$\phi_i = \tan^{-1}\left[\frac{y_r}{x_r}\right]. \tag{3}$$

The total path length from the feed to the reflectarray aperture is the sum of the distance from the feed to a point on the backscatter surface and the distance from that point to the corresponding point on the reflectarray with the rays satisfying Snell's

law on the backscatter surface. In the analysis of backscatter, it is desirable to find a unit vector that is normal to the local tangent at the surface reflection point

$$\hat{n} = \frac{\nabla\left[z - f(z')\right]}{\left|\nabla\left[z - f(z')\right]\right|}. \tag{4}$$

With the help of Snell's law of reflection, the reflected angle for the backscatter can be expressed in (5).

$$\theta_r = 2\cos^{-1}\left[-\frac{\vec{\rho}_i}{|\vec{\rho}_i|}\cdot\hat{n}\right] - \theta_i. \tag{5}$$

The differential path length (ΔL_{mn}) and the phase delay ($\Delta\Phi_{mn}$) for the *mn*-th reflectarray element are given by

$$\Delta L_{mn} = |\bar{\rho}_i| + \frac{z_b - f}{\sin\theta_r} - |\vec{r}_{mn,i}|, \tag{6}$$

$$\Delta\Phi_{mn} \text{ in degree} = \left[(1-N)k_0\Delta L_{mn}\right]\frac{360}{2\pi}, \tag{7}$$

where N is integer. The above indicates that the compensating phase can be repeated every 360 deg, and the portion that is an integer multiple of 360 deg can be deleted.

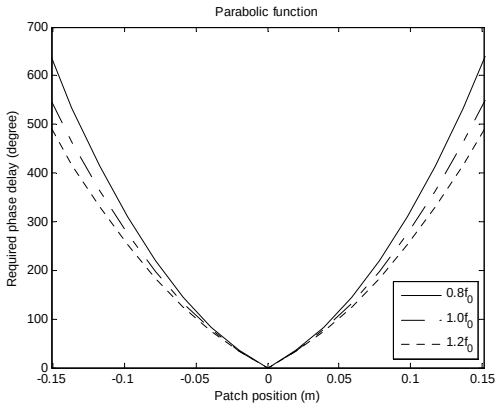

Fig. 3 Desired phase delay.

The required phase delays of all elements are calculated and will be used to design the dimension of the reflectarray elements as shown in Fig. 3 with various center frequencies (f_0 = 10 GHz). These phase delays are duplicated the same radiating aperture as parabolic backscatter, which its geometrical function can be written as

$$f(z') = -\frac{x_b^2 + y_b^2}{4f} - f. \tag{8}$$

2.2 Element Characterization

The most important and critical segment of the reflectarray design is its element characterization. To compensate for above phase delays, the elements must have corresponding phase advancements designed. Its phase change versus element change (patch size, etc.) must be calibrated correctly. If the element design is not optimized, it will not scatter the signal from the feed effectively to form an efficiently far-field beam. In this paper, the phase calibration technique is to use a full-wave method of moment and the infinite-array approach to model the effect of the finite grounded dielectric substrate underlying the single radiator [7],[9].

In order to determine the solution used to design and analyze a microstrip reflectarray, we assume an incident plane wave with an electric field of the form

$$\bar{E}^{inc} = \bar{E}_0 e^{-jk_0(xu_i + yv_i - zw_i)}, \tag{9}$$

where the complex vector $\bar{E}_0$ defines the amplitude and direction of the incident field and

$$u_i = -\sin\theta_i\cos\phi_i,\ v_i = -\sin\theta_i\sin\phi_i,\ w_i = -\cos\theta_i. \tag{10}$$

The phase reference for this and the following fields are at the bottom of substrate. In the absence of array elements, the reflected field from the dielectric substrate and ground plane can be expressed as

$$\begin{bmatrix} E_\theta^{ref} \\ E_\phi^{ref} \end{bmatrix} = \begin{bmatrix} R_{\theta\theta} & 0 \\ 0 & R_{\phi\phi} \end{bmatrix}\begin{bmatrix} E_{0\theta} \\ E_{0\phi} \end{bmatrix} e^{jk_0(xu_i + yv_i - z\cos\theta_i)} = \bar{\bar{R}}\cdot\bar{E}_0 e^{jk_0(xu_i + yv_i - z\cos\theta_i)}, \tag{11}$$

where $R_{\theta\theta}$ and $R_{\phi\phi}$ are the plane wave reflection coefficients as given in [9].

The presence of the elements gives rise to an additional scattered field component that are given by

$$\begin{bmatrix} E_\theta^{scat} \\ E_\phi^{scat} \end{bmatrix} = \begin{bmatrix} S_{\theta\theta} & S_{\theta\phi} \\ S_{\phi\theta} & S_{\phi\phi} \end{bmatrix}\begin{bmatrix} E_{0\theta} \\ E_{0\phi} \end{bmatrix} e^{jk_0(xu_i + yv_i - z\cos\theta_i)} = \bar{\bar{S}}\cdot\bar{E}_0 e^{jk_0(xu_i + yv_i - z\cos\theta_i)}. \tag{13}$$

Evaluation of the total scattered field from the microstrip reflectarray is based on the assumption that each element of the finite reflectarray scatters as a Huygens source with reflection coefficient equivalent to the total reflection coefficient of an infinite array of similar elements.

$$\bar{E}^{tot} = \begin{bmatrix} R_{\theta\theta} + S_{\theta\theta} & S_{\theta\phi} \\ S_{\phi\theta} & R_{\phi\phi} + S_{\phi\phi} \end{bmatrix}\begin{bmatrix} E_{0\theta} \\ E_{0\phi} \end{bmatrix} e^{jk_0(xu_i + yv_i - z\cos\theta_i)}. \tag{14}$$

From (14), the reflection phase required for the design to compensate above phase delays can be found from this result.

The scattering coefficients ($\bar{\bar{S}}$), which defined in (13) are found by using a full-wave solution. The method of moment impedance matrix for infinite array of uniform elements can be computed as

$$Z_{ij} = -\frac{1}{s^2}\sum_{m=-\infty}^{m=\infty}\sum_{n=-\infty}^{n=\infty}\tilde{J}_i(k_x', k_y')\cdot\bar{\bar{G}}(k_x', k_y')\cdot\tilde{J}_j(k_x', k_y'), \quad (15)$$

where s is center-to-center elements spacing in both x and y directions, $\tilde{J}$ is the Fourier transform of the ith expansion mode current, and $\bar{\bar{G}}$ is the dyadic Green's function for the dielectric substrate.

The voltage vector elements can be expressed in (16)

$$V_i = \bar{J}_{s0}\cdot\bar{\bar{G}}(k_0 u_i, k_0 v_i)\cdot\bar{J}_i(k_0 u_i, k_0 v_i), \quad (16)$$

where

$$\bar{J}_{s0} = \frac{-2}{\eta_0}\begin{bmatrix}\hat{x}(E_{0\theta}\cos\phi_i - E_{0\phi}\cos\theta_i\sin\phi_i)\\ +\hat{y}(E_{0\theta}\sin\phi_i - E_{0\phi}\cos\theta_i\cos\phi_i)\end{bmatrix}. \quad (17)$$

Fig. 4 shows simulated results of reflection phase of infinite array. The obtained results indicated that, if the element size L is excessively small, either the reflection phase cannot be made to cover the full required 0° to 360° phase range, or it changes excessively fast around the element resonance. This available phase shift rang is limited by the reflectarray antenna bandwidth (around 4%).

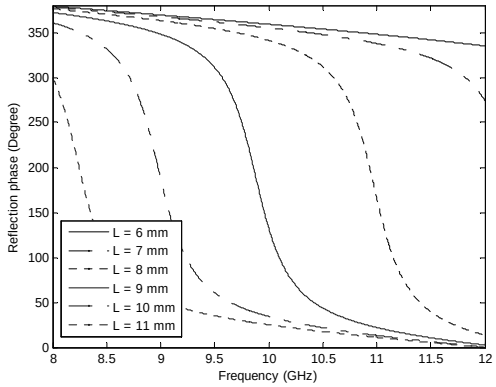

Fig. 4 Reflection phase of total reflected field from an infinite array of microstrip patches.

3 Radiation Pattern Calculation

With the compensating phases of all elements known, the far-field radiation patterns can be calculated by the conventional array theory [8], where the radiations of all elements are summed together as follows. Considering a planar array consisting of $M \times N$ elements that are nonuniformly illuminated by a low-gain feed, the reradiated field from the patches in an arbitrary direction, $\hat{u}$, will be of the form

$$E(\hat{u}) = \sum_{m=1}^{M}\sum_{n=1}^{N} F(\vec{r}_{mn}\cdot\hat{a}_z)\cdot A(\vec{r}_i\cdot\hat{u}_r)\cdot A(\hat{u}\cdot\hat{u}_r) \cdot\exp\left[-jk_0\left(|\vec{r}_{mn}| + \vec{r}_i\cdot\hat{u}\right) - j\Delta\Phi_{mn}\right], \quad (9)$$

where F is the feed pattern function, A is the reflectarray element pattern function, $\vec{r}_i$ is the vector from the centre of reflectarray to mn-th element, $\hat{u}_r$ is the unit vector of reflected field, and $\Delta\Phi_{mn}$ is the required compensating phase of the mn-th element calculated by (7).

4 Design Considerations of Broad-Beam Microstrip Reflectarray and Experimental Results

The reflectarray of 30 cm dimension is designed and measured with a standard X-band horn feed, which is placed in front of reflectarray surface and its radiation pattern is shown in Fig.5. The cell elements of reflectarray are printed on a TACONIC substrate with thickness 0.762 mm and permittivity ε_r = 2.33. The centre-to-centre elements spacing is fixed at a distance $s = 0.6\lambda_0$ in both x and y directions.

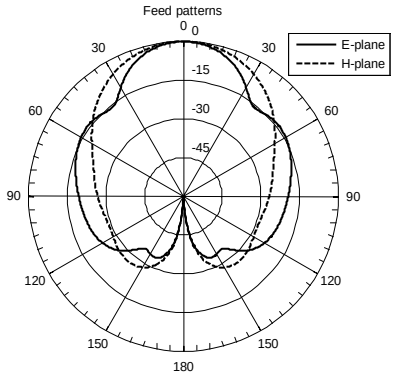

Fig. 5 Radiation pattern of standard X-band Horn.

It has been easy to calculate efficiency for a feed horn pattern and reflectarray due to illumination taper and spillover as given in [8],[9]. However, there are several other factors that can significantly reduce efficiency. Because the feed horn and its supporting structures are in the beam direction of the reflectarray, therefore, some part of the radiation is blocked. Also, considering the aperture, taper, spillover, and feed blockage efficiencies relations versus distance between the feed and the reflectarray to a dimension (*f/D*) ratio are calculated and plotted in Fig. 6. As in the case of front feed reflector, there is an optimum value of *f/D* that maximizes aperture

efficiency for a given feed pattern. This maximum value is slightly lower than the optimum aperture efficiency for the parabolic case because of a slightly lower taper efficiency. When the feed blockage efficiency is considered, maximum aperture efficiency is reduced and feed distance is changed while a reflectarray dimension is fixed. In this paper, we have investigated the influence of the feed position on the -3 dB beamwidth (HPBW) and gain performance before the reflectarray will be fabricated. Where the first feed distance *f* is located at point that maximizes aperture efficiency (61%).

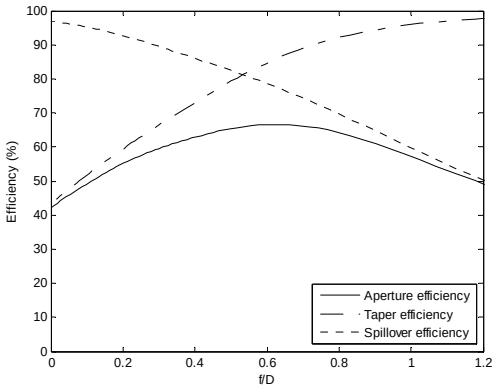

(a)

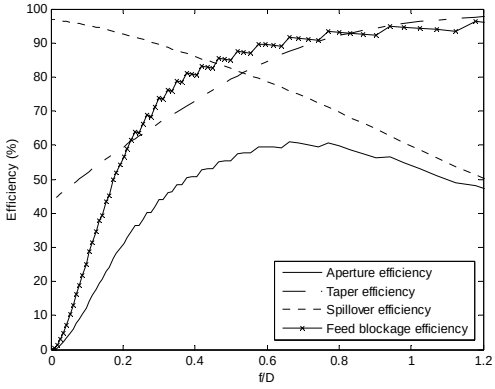

(b)

Fig. 6 Reflectarray efficiency (a) without and (b) with considering the feed blockage efficiency.

In order to optimize the feed position of broad-beam reflectarray, the calculated results as shown in Fig. 7 indicate the different radiation patterns for the various feed positions. The total re-radiation field is computed as the summation of all the contributions from each array element. The prescribed field requirements have been satisfied by an appropriate choice of the radiating patches selected from the complex design curves obtained in the analysis stage.

The steepness of the pattern edges and their angular positions confirmed that the antenna efficiently illuminates the target area to be covered (±65°). The obtained radiation patterns are different due to phase of reflectarray elements, which are duplicated the same radiating aperture as parabolic backscatter. Moreover, the ripple appeared on the top of each pattern can indicate that, if the feed distance is reduced then the ripple is increased. Away from the main beam, the phase center may move around and appear as multiple points, as stray reflections and surface currents affect the radiation pattern. Because of phase change versus element change, each feed distance provides different characteristics such as HPBW and gain, which are reported in Table 1.

Table 1
Characteristics of reflectarray.

Feed distance	HPBW (degree)	Gain (dB) at θ=0°	Maximum gain (dB)
f - 10% f	158	1.43	8.81
f - 5% f	151	-6.13	9.35
f	144	0.32	10.75
f + 5% f	144	1.99	11.10
f + 10% f	145	1.52	12.16

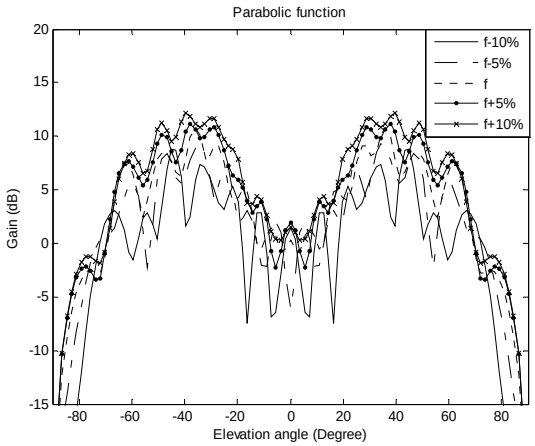

Fig. 7 Radiation pattern in H-plane of broad-beam reflectarray for the various feed positions.

From Table 1, it is found that the HPBW of reflectarrays are different when the feed distance is varied. For average consideration, it is apparent that the feed position not far away in distance from reflectarray provides the widest beamwidth. Since the maximum gain is strongly coincided with the HPBW i.e., the narrower the beamwidth the higher the maximum gain and vice versa. However, the reflection surface for reflectarray elements are placed position near the centre of backscatter. Thus, the enlargement of the feed distance yields the lowest feed blockage efficiency and the highest gain

at $\theta = 0°$.

However, it is generally observed that when the antenna beam is enlarged, the antenna gain is reduced. With the optimum design requirement, the feed distance is chosen at 25 cm, which caused the maximum aperture efficiency to be reduced approximately 2% but its gain is increased. In Fig. 8, the prototype of reflectarray antenna is realized following this approach and measured. From the measurement as shown in Fig. 9, the antenna has the HPBW of 145° and maximum gain of 13 dB at the frequency of 10 GHz. The measured gain pattern have been corrected by 2 dB for loss in the waveguide feed transition. An additional cause of asymmetry observed in the patterns is fabrication tolerance. The computed performances of this reflectarray are in good agreement with those of the measured prototype.

5 Conclusions

A broad-beam microstrip reflectarray designed from square patches has been presented. The optimized feed distance is calculated from the aperture efficiency with considering feed blockage efficiency and has investigated the influence of the feed position on the -3 dB beamwidth and gain performance. The prescribed field requirements have been satisfied by an appropriate choice of the radiating patches array selected from the complex design curves obtained in the analysis stage. Simulation of this reflectarray demonstrates that increasing of feed distance can enhance maximum gain but its HPBW is reduced. From all the aforementioned of radiation characteristics, it can be summarized that if we need to improve gain performance for broad-beam reflectarray antenna, an optimum feed distance would provide a feed radiation pattern which completely illuminates the reflectarray with minimal spillover.

References:

[1] Peter F.M. Smulder, S. Khusial, and H.A.J. Herben, A shaped reflector antenna for 60-GHz indoor wireless LAN access points, *IEEE Trans. on Verhicular Technology*, Vol. 50, No. 2, 2001, pp. 584-591.

[2] R. Wongsan, V. Thaivirot, Synshesis of radiation pattern of variety of shaped backscatters using physical optic, *Proc. of ECTI-CON 2006*, Vol. 1, 2006, pp. 155-158.

[3] R.E. Munson, H.A. Haddad, and J.W. Hanlen, Microstrip reflectarray for satellite communications and RCS enhancement or reduction, *U.S. patent 4 684 952*, 1987.

[4] D.C. Chang and M.C. Huang, Multiple-polarization microstrip reflectarray antenna with high efficiency and low cross-polarization, *IEEE Trans. on Antenna and Propag.*, Vol.43, No.8, 1995, pp. 829-834.

[5] J.A. Encinar, Design of two-layer printed reflectarrays using patches of variable size, *IEEE Trans. on Antennas and Propag.*, Vol. 49, 2001, pp.1403-1410.

[6] D.M. Pozar, S.D. Targonski, and R. Pokuls, A shaped-beam microstrip patch reflectarray, *IEEE Trans. on Antenna and Propag*., Vol.47, Issue 7, 1999, pp. 1167-1173.

[7] P. Krachodnok and R. Wongsan, Design of microstrip reflectarray antenna using backscattering technique, *Proc. of ITC-CSCC 2006*, Vol. 3, 2006, pp. 513-516.

[8] J. Huang, Analysis of a microstrip reflectarray antenna for microspacecraft applications, *The Telecommunications and Data Acquisition Progress Report 42-120*, 1995, pp. 153-173.

[9] D.M. Pozar, S.D. Targonski, and H.D. Syrigos Design of millimeter wave microstrip reflectarray, *IEEE Trans. on Antenna and Propagation*, Vol.45, No.2, 1997, pp. 287-296.

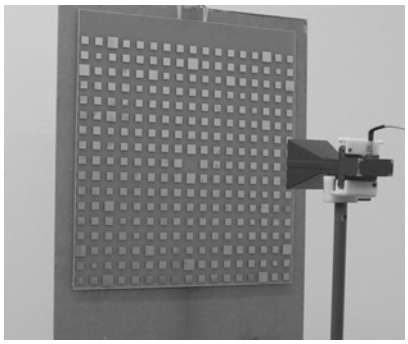

Fig. 8 Reflectarray prototype.

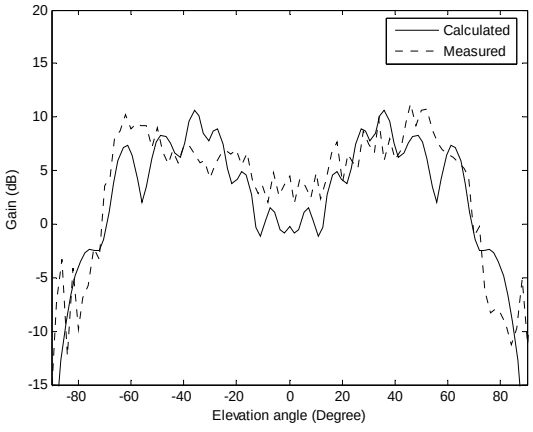

Fig. 9 Calculated and measured radiation patterns of designed reflectarray at 10 GHz.